Journal of Power Sources 257 (2014) 221–229

Contents lists available at ScienceDirect

Journal of Power Sources

journal homepage: www.elsevier.com/locate/jpowsour

Sulfonated poly(ether ether ketone)/mesoporous silica hybrid membrane for high performance vanadium redox flow battery

Zhaohua Li [a,b], Wenjing Dai [a], Lihong Yu [c], Jingyu Xi [a,*], Xinping Qiu [a,b,**], Liquan Chen [a,b]

[a] Lab of Advanced Power Sources, Graduate School at Shenzhen, Tsinghua University, Shenzhen 518055, China
[b] Key Lab of Organic Optoelectronics and Molecular Engineering, Department of Chemistry, Tsinghua University, Beijing 100084, China
[c] Department of Chemistry, The University of Hong Kong, Pokfulam Road, Hong Kong, China

HIGHLIGHTS

- SPEEK/SBA-15 (S/SBA-15) hybrid membranes are used in vanadium redox flow battery.
- S/SBA-15 hybrid membranes are dense and homogeneous with no visible hole.
- Membranes show good property trends for the interaction between SPEEK and SBA-15.
- S/SBA-15 20 membrane shows highest efficiency and highly stable cycle performance.

GRAPHICAL ABSTRACT

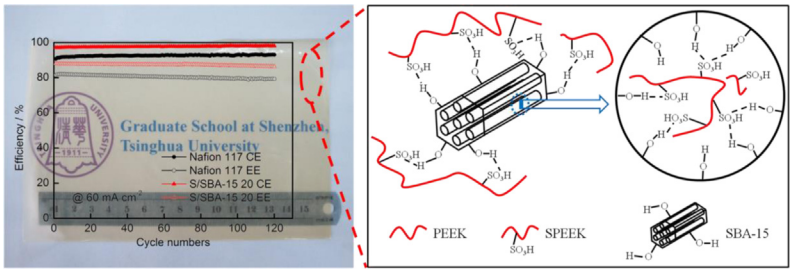

ARTICLE INFO

Article history:
Received 11 December 2013
Received in revised form
17 January 2014
Accepted 28 January 2014
Available online 8 February 2014

Keywords:
Vanadium redox flow battery
Sulfonated poly(ether ether ketone)
Mesoporous silica
Hybrid membrane

ABSTRACT

Hybrid membranes of sulfonated poly(ether ether ketone) (SPEEK) and mesoporous silica SBA-15 are prepared with various mass ratios for vanadium redox flow battery (VRB) application and investigated in detail. The hybrid membranes are dense and homogeneous with no visible hole as the SEM and EDX images shown. With the increasing of SBA-15 mass ratio, the physicochemical property, VO^{2+} permeability, mechanical property and thermal stability of hybrid membranes exhibit good trends, which can be attributed to the interaction between SPEEK and SBA-15. The hybrid membrane with 20 wt.% SBA-15 (termed as S/SBA-15 20) shows the VRB single cell performance of CE 96.3% and EE 88.1% at 60 mA cm^{-2} due to its good balance of proton conductivity and VO^{2+} permeability, while Nafion 117 membrane shows the cell performance of CE 92.2% and EE 81.0%. Besides, the S/SBA-15 20 membrane shows stable cell performance of highly stable efficiency and slower discharge capacity decline during 120 cycles at 60 mA cm^{-2}. Therefore, the SPEEK/SBA-15 hybrid membranes with optimized mass ratio and excellent VRB performance can be achieved, exhibiting good potential usage in VRB systems.

1. Introduction

To fulfill the rapid increasing of global usage of renewable energy such as wind and solar energy, it is urgent to develop a safe and effective electrical energy storage (EES) to surmount the instability and intermittence natures of the renewable energy [1,2]. As a sort of rechargeable battery, vanadium redox flow battery (VRB), which is pioneered and developed by M. Skyllas-Kazacos et al. [3–6], has been considered to be a promising candidate for

* Corresponding author. Tel.: +86 755 2603 6436; fax: +86 755 2603 6181.
** Corresponding author. Lab of Advanced Power Sources, Graduate School at Shenzhen, Tsinghua University, Shenzhen 518055, China. Tel./fax: +86 10 6279 4234.
E-mail addresses: xijingyu@gmail.com (J. Xi), qiuxp@tsinghua.edu.cn (X. Qiu).

http://dx.doi.org/10.1016/j.jpowsour.2014.01.127
0378-7753/

stationary EES due to its features like long cycle life, low cost, flexible design and high energy efficiency [7–9]. The conventional VRB, with the standard open circuit cell voltage of 1.26 V, employs VO^{2+}/VO_2^+ and V^{2+}/V^{3+} dissolved in sulfuric acid as the positive and negative electrolytes respectively, carbon materials as the electrodes, and ion exchange membranes (IEMs) as the separators [10,11]. To date, many progresses have been reported in high concentration and stability electrolytes, high activity electrodes, high performance membranes, monitoring, modeling, etc [12–20]. However, the lack of low-cost membrane accompanied with low vanadium ion permeability and high VRB performance is limiting the commercialization of VRB.

The commonly used IEMs in VRB are perfluorosulfonic polymer such as Nafion membranes (DuPont) owing to their high proton conductivity and excellent chemical, electrochemical stability. However, the Nafion membranes possess high vanadium ion permeability accompanied with corresponding problems like low efficiency and fast capacity decline [21]. Though great deal of modified Nafion membranes with improving VRB performances have been prepared and researched [22–29], the costs of these membranes for large-scale VRB systems are still extremely high. The modified Nafion membranes are not suitable for the commercialization of VRB systems. Therefore, alternative low-cost membrane with high performance is imminently required for the widely usage of VRB.

Owing to the feature of low cost, the nonionic porous membranes have been researched for VRB applications recently [30–32]. The porous membrane could separate vanadium ions from protons via pore size exclusion due to the differences in stokes radius, causing low vanadium ion permeability and relatively high VRB performance. However, it is hard to control the uniform morphology of porous membrane, and the heterogeneous morphology would highly affect the VRB performance. Further optimization should be proposed to make homogeneous morphology of porous membrane and higher VRB performance.

In recent years several research groups have tried to develop anion exchange membranes (AEMs) as alternative low-cost materials for VRB application [33–36]. The low vanadium ion permeability of AEM can be due to the Donnan exclusion effect between cationic groups in AEM and vanadium ions. Furthermore, the decrease of VO_2^+ adsorbed in AEM could be postulated to reduce the chemical degradation of membrane. However, the much lower ionic conductivity of AEM, which is owing to the slower mobility of sulfate anion served as the major charge carrier, would lead to lower voltage efficiency and energy efficiency, making AEM unsuitable for VRB high current density application. Therefore, the cation exchange membranes (CEMs) are still drawing considerable attention for the widely usability in VRB systems.

As one kind of CEMs, the sulfonated poly aromatic membranes have been assessed in VRB systems as candidates for the substitution of Nafion membranes [37–41]. In these sulfonated poly aromatic membranes, the sulfonated poly(ether ether ketone) (SPEEK) membrane has received more attention due to its easy preparation and high VRB performance. However, high degree of sulfonation (DS) SPEEK membrane would cause high vanadium ion permeability, low membrane stability and VRB performance, which are limiting its further application in VRB. Thus the inorganic doping [40] or polymer blending [17] modification of high DS SPEEK membrane could be used to prepare composite membranes with high VRB performance.

The mesoporous silica SBA-15 could be used in many fields due to its ordered mesoporous pore structure and high mechanical, thermal stability [42,43]. As excellent inorganic filler, SBA-15 modified with high DS SPEEK hybrid membranes would possess low vanadium ion permeability and high membrane stability by the postulate of hydrogen bond formed between $-SO_3H$ group from SPEEK and $-OH$ group on SBA-15, resulting in low-cost and high performance membranes for VRB. In this work, the SPEEK/SBA-15 hybrid membranes were prepared by solution casting method. The morphology, physicochemical property, VO^{2+} permeability, mechanical property, thermal stability and VRB single cell performance of the hybrid membranes were investigated and discussed in detail. The interaction mechanism between SPEEK and SBA-15 was also proposed.

2. Experimental

2.1. Materials and membrane preparation

Poly(ether ether ketone) (PEEK) (Victrex, PEEK 450P) was washed and then dried. Sulfonated poly(ether ether ketone) (SPEEK) with ion exchange capacity (IEC) of 2.12 mmol g^{-1} (DS = 0.74) was prepared according to our previous report [17], and its chemical structure was shown in Scheme 1. Mesoporous silica SBA-15 (Pore Diameter: 9 ~ 10 nm; BET: 800 $m^2\ g^{-1}$) was purchased from China Nanjing XFNano Material Tech Co., Ltd. Nafion 117 membrane was purchased from Dupont company. Other reagents were all analytical grade and used without further purification.

The SPEEK/SBA-15 hybrid membranes were prepared by solution casting method as following procedures. First, predetermined weight of SBA-15 was added in 10 mL *N*,*N*-Dimethylformamide (DMF) to make a homogeneous suspension via 30 min of ultrasonic dispersion. Then the corresponding weight of SPEEK was added in the SBA-15 homogeneous suspension and magnetic stirred for 24 h to form a 15 wt./vol.% homogeneous casting solution. The casting solution was cast on a clean plate glass and dried at 60 °C over night, then dried at 80 °C for 24 h in vacuum. The membrane was peeled off from the plate glass by immersing the plate glass into deionized water. Finally, the membrane was immersed in 1 mol L^{-1} H_2SO_4 solution for 24 h, then immersed in deionized water for 48 h to remove the residual acid solution, and stored in deionized water.

The SPEEK/SBA-15 hybrid membranes with various SBA-15 mass ratios are termed as S/SBA-15 *X*, where *X* is the SBA-15 mass ratio. For example, the S/SBA-15 20 is a membrane with 20 wt.% SBA-15 and 80 wt.% SPEEK. Besides, the Nafion 117 membrane served as reference membrane was pretreated by the standard method according to our previous report [17].

2.2. Membrane characterization

2.2.1. Morphology

The morphology and EDX of membrane cross-section were confirmed by SEM (Hitachi S-4800, Japan). The sample membrane prepared for the morphology observation was obtained by breaking the sample membrane in liquid nitrogen and then coating it with gold.

2.2.2. Physicochemical property

The residual water on the surface of sample membrane was wiped off with filter papers, following with the quick measurements of size and weight. Then the sample membrane was dried at 100 °C in vacuum for 12 h and measured as soon as possible. The above-mentioned procedures were repeated at least three times to gain a good data reproducibility. The water uptake and swelling ratio of sample membrane were calculated by following equations:

$$\text{Water uptake}\ (\%) = \frac{W_{wet} - W_{dry}}{W_{dry}} \times 100\% \quad (1)$$

$$\text{Swelling ratio}\ (\%) = \frac{L_{wet} - L_{dry}}{L_{dry}} \times 100\% \quad (2)$$

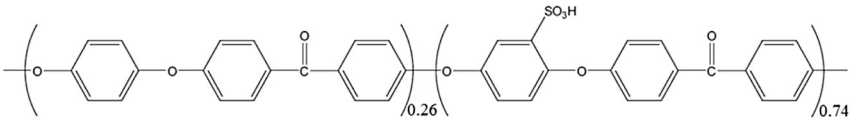

Scheme 1. The chemical structure of SPEEK (DS = 0.74 in this work).

where W_{wet} and W_{dry} are the weight of wet and dry sample membrane respectively, L_{wet} and L_{dry} are the length of wet and dry sample membrane respectively.

The ion exchange capacity (IEC) of sample membrane was determined by classical titration. Employing 50 mL saturated NaCl solution as the ion exchange agent, the amount of H^+ exchanged from the sample membrane was determined by titrating with 0.1 mol L^{-1} NaOH solution, using phenolphthalein as indicator. The IEC of sample membrane was calculated by following equation:

$$\mathrm{IEC}\left(\mathrm{mmol\ g^{-1}}\right) = \frac{C_{\mathrm{NaOH}} \times V_{\mathrm{NaOH}}}{W_{\mathrm{dry}}} \tag{3}$$

where IEC is the ion exchange capacity, C_{NaOH} and V_{NaOH} are the molarity and the consumed volume of NaOH solution, respectively. The degree of sulfonation (DS) of SPEEK was calculated according to the IEC result and our previous report [17], with the result of DS = 0.74 in this work.

The measurement of proton conductivity of sample membrane was carried out via the two-probe electrochemical impedance spectroscopy (EIS) with a PARSTAT 2273 electrochemical station (USA, AMETEK, Inc.) according to our previous reports [10,17]. The proton conductivity of sample membrane was calculated by following equation:

$$\sigma\left(\mathrm{mS\ cm^{-1}}\right) = \frac{L}{A \times R} \tag{4}$$

where σ is the proton conductivity, A and L are the effective area and thickness of sample membrane, R is the sample membrane resistance.

2.2.3. VO^{2+} permeability

The VO^{2+} permeability of sample membrane was determined according to our previous reports [17,25]. The effective area of sample membrane was 7 cm^2. The left reservoir was filled with 38 mL 1.5 mol L^{-1} $VOSO_4$ in 3 mol L^{-1} H_2SO_4 solution, and the right reservoir was filled with 38 mL 1.5 mol L^{-1} $MgSO_4$ in 3 mol L^{-1} H_2SO_4 solution. Both solutions were magnetic stirred throughout the measurement. 3 mL solution of the right reservoir was collected and measured by a UV–vis spectrometer (752S, Leng Guang Tech., China) at regular time intervals, and then was laid back in the right reservoir. The VO^{2+} permeability of membrane was calculated by following equation:

$$V_{\mathrm{R}}\frac{\mathrm{d}C_{\mathrm{R}}(t)}{\mathrm{d}t} = A\frac{P}{L}(C_{\mathrm{L}} - C_{\mathrm{R}}(t)) \tag{5}$$

where V_R is the solution volume of right reservoir, C_L and $C_R(t)$ are the VO^{2+} concentration in the left reservoir and right reservoir respectively, A and L are the effective area and thickness of the sample membrane respectively, P is the VO^{2+} permeability.

2.2.4. Mechanical property

The mechanical property of air-dry sample membrane was measured by CMT5504 equipment (Suns Aspect Technology Co., Ltd., China). The sample membrane was cut into 70 mm × 10 mm. The gauge length and tensile speed were 30 mm and 2 mm min^{-1}, respectively.

2.2.5. Thermal stability

Thermogravimetric analysis (TGA) conducted on a TA Q5000IR thermal analyzer was used to assess the thermal stability of membranes. Before testing, the sample membrane was preheated at 120 °C for 10 min to remove any residual moisture and solvent, and then the sample membrane was cooled to 100 °C and reheated to 800 °C at a heating rate of 10 °C min^{-1} in N_2 gas atmosphere.

2.3. VRB single cell test

The VRB single cell used in this work was assembled by sandwiching a membrane with two heat treated graphite felts (thickness of 5 mm) served as electrodes, clamped by two graphite polar plates served as current collectors [17]. The effective area of membrane was 5 × 5 cm^2. All these components were fixed between two thick flat plastic plates. Two 50 mL 2.0 mol L^{-1} VO^{2+}/V^{3+} (mol:mol = 1:1) in 2.0 mol L^{-1} H_2SO_4 solutions were used as positive and negative electrolytes, respectively. The electrolyte was cyclically pumped into the corresponding half cell in airtight pipe lines by a peristaltic pump. The VRB single cell performance was recorded by the Neware CT-3008W (5V6A) battery testing system.

The charge–discharge test was conducted at current densities from 40 to 80 mA cm^{-2}. The cut-off voltages were set at 1.65 V and 0.8 V respectively to avoid the corrosion of graphite felts and graphite polar plates.

The VRB single cell was firstly charged to 50% state of charge (SoC) at the current density of 60 mA cm^{-2}. Then the self-discharge test immediately began and stopped until the single cell open circuit voltage (OCV) was below 0.8 V.

The cycle life test was carried out at the constant current density of 60 mA cm^{-2} with the cut-off voltages setting at 1.65 V and 0.8 V, respectively.

The coulombic efficiency (CE), voltage efficiency (VE) and energy efficiency (EE) of VRB single cell were calculated by following equations:

$$\mathrm{CE}\ (\%) = \frac{\int_0^t I_{\mathrm{d}}\mathrm{d}t}{\int_0^t I_{\mathrm{c}}\mathrm{d}t} \times 100\% \tag{6}$$

$$\mathrm{EE}\ (\%) = \frac{\int_0^t V_{\mathrm{d}} I_{\mathrm{d}}\mathrm{d}t}{\int_0^t V_{\mathrm{c}} I_{\mathrm{c}}\mathrm{d}t} \times 100\% \tag{7}$$

$$\mathrm{VE}\ (\%) = \frac{\mathrm{EE}}{\mathrm{CE}} \times 100\% \tag{8}$$

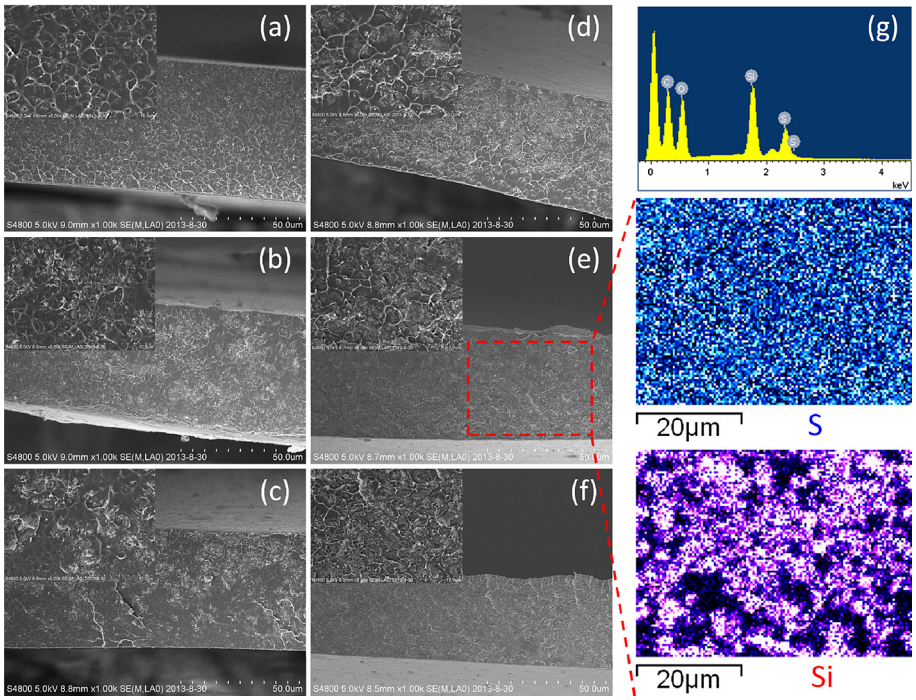

Fig. 1. Cross-section morphology of membranes: (a) SPEEK, (b) S/SBA-15 5, (c) S/SBA-15 10, (d) S/SBA-15 15, (e) S/SBA-15 20 and (f) S/SBA-15 25; and EDX image: (g) S/SBA-15 20.

where I_c and I_d are the charging current and discharging current respectively, V_c and V_d are the charging voltage and discharging voltage respectively.

3. Results and discussion

3.1. Morphology

The morphology of hybrid membranes is confirmed by SEM and the images are illustrated in Fig. 1. The cross-sections in Fig. 1(a–f) demonstrate that the hybrid membranes are dense and homogeneous with no visible hole. The insets on the upper left of Fig. 1(a–f) demonstrate that the SBA-15 is uniformly dispersed in the matrix of hybrid membrane. Besides, the amount of SBA-15 showed in the insets increases with the increasing of SBA-15 mass ratio. Furthermore, the dispersion of SPEEK and SBA-15 is investigated by EDX and shown in Fig. 1g. It can be seen that the element S (blue color (in the web version)) originated from the $-SO_3H$ groups and the element Si (red color) originated from the SBA-15 are uniformly distributed in the cross-section of S/SBA-15 20 membrane, indicating that the hybrid membranes are homogeneous.

3.2. Physicochemical property

The physicochemical property of various membranes is illustrated in Fig. 2, and the corresponding data is listed in Table 1. As shown in Fig. 2, the value of physicochemical property generally decreases with the increasing of SBA-15 mass ratio.

The water uptake in hybrid membrane plays a remarkable role in the proton conductivity. Higher water uptake generally improves the proton conductivity with the facilitating of $-SO_3H$ groups dissociation and proton migration [44]. Whether the calculation of water uptake is based on the weight of entire sample membrane (the red line (in the web version) in Fig. 2a) or the weight of SPEEK content in sample membrane (the blue line in Fig. 2a), the water uptake of hybrid membranes always decreases with the increasing of SBA-15 mass ratio. This phenomenon could be due to the interaction between SPEEK and SBA-15 by the hydrogen bond formed between $-SO_3H$ group in SPEEK and $-OH$ group on SBA-15 [45] as shown in Scheme 2. With the increasing of SBA-15 mass ratio, the interaction would be stronger and the hydrophilic domain formed by $-SO_3H$ groups [46] would be less, which would further restrain the water absorption of hybrid membrane. Normally, lower water uptake would lead to lower vanadium ion permeability and higher VRB performance.

As shown in Fig. 2b, the swelling ratio decreases with the increasing of SBA-15 mass ratio. Moreover, the decreasing extent of swelling ratio is larger than the increasing extent of SBA-15 mass ratio, which indicates that the existence of interaction between SPEEK and SBA-15. The explanation of this phenomenon may be due to the interaction between SPEEK and SBA-15, which consist of the filling mesoporous pores of SBA-15 with SPEEK and the hydrogen bond formed between SPEEK and SBA-15 as shown in Scheme 2. Normally, smaller swelling ratio would lead to better mechanical property and membrane stability during the actual VRB operation. The more stable VRB performance and slower capacity decline could also be achieved with lower swelling ratio.

It can be seen that the ion exchange capacity (IEC) of hybrid membranes decreases linearly with the increasing of SBA-15 mass ratio as shown in Fig. 2c, which means that the IEC of hybrid membrane could be easily controlled by varying the SBA-15 mass ratio. Although the interaction between SPEEK and SBA-15 exists as discussed above, the IEC result reveals that the SBA-15 has no hindrance during the ion exchange process. This phenomenon of no hindrance would be undoubtedly advantageous to the proton conductivity.

The proton conductivity of hybrid membranes is presented in Fig. 2d. The proton conductivity of membrane could be affected by various factors, especially water uptake and IEC [45]. As the water uptake and IEC results shown above, the proton conductivity of hybrid membranes with a similar decreasing trend as shown in Fig. 2d could be expected. The proton conductivity decreases slowly

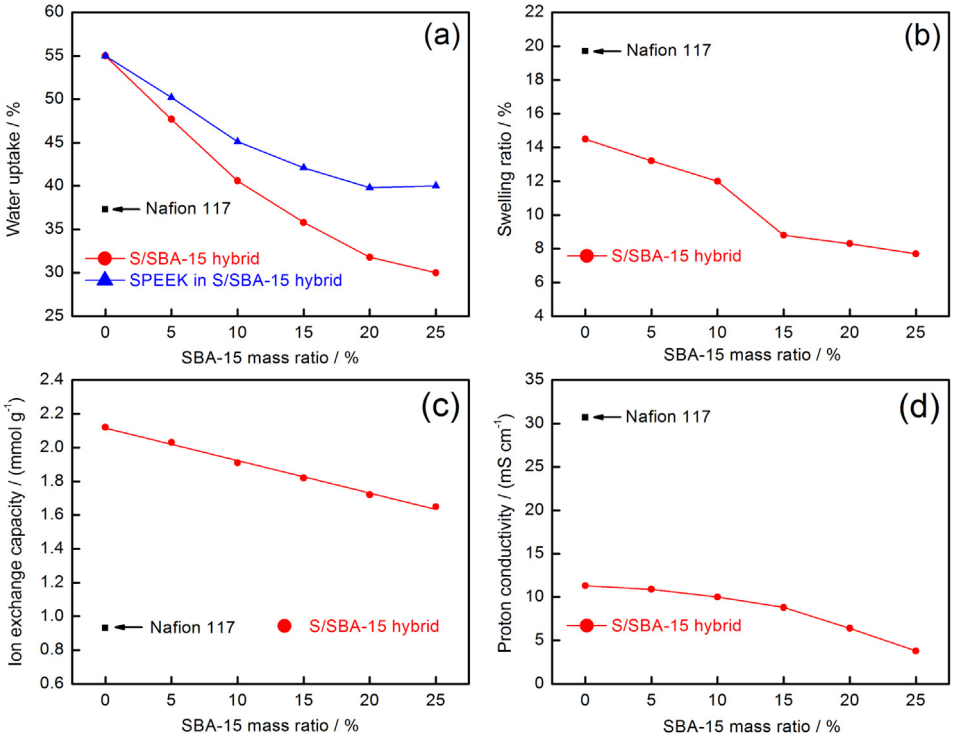

Fig. 2. Physicochemical property of Nafion 117, SPEEK and hybrid membranes.

at first, and then drops quickly after S/SBA-15 15 membrane, which is due to the dual decreases of water uptake and IEC. Suitable membrane proton conductivity could result in good balance between vanadium ion permeability (coulombic efficiency) and resistance (voltage efficiency), causing better VRB single cell performance (higher energy efficiency).

3.3. VO^{2+} permeability

The VO^{2+} permeability data of various membranes is listed in Table 1. The VO^{2+} permeability values of hybrid membranes (from 18.4 to 6.2 $\times$ 10^{-7} cm^2 min^{-1}) are smaller than Nafion 117 membrane (32.2 $\times$ 10^{-7} cm^2 min^{-1}), which would lead to lower self-discharge rate and higher coulombic efficiency. The lower VO^{2+} permeability of hybrid membranes could be explained by following comment as elsewhere reported [46]. Generally, the SPEEK membrane has smaller hydrophilic/hydrophobic separation and higher dispersed $-SO_3H$ groups, causing the narrow and branched water filled channels compared with Nafion membrane. Thus the migration of vanadium ion in SPEEK membranes is slower. Moreover, the addition of SBA-15 would further separate the hydrophilic domain in the hybrid membranes, which increases the difficulty of vanadium ion permeation, leading to lower and good trend of VO^{2+} permeability.

3.4. Mechanical property and thermal stability

The mechanical property data of various membranes is listed in Table 1. It can be seen that the breaking strength and the young modulus of hybrid membranes are higher than Nafion 117 membrane, which reveals that the hybrid membranes possess better mechanical property. The young modulus of hybrid membranes constantly increases with the increasing of SBA-15 mass ratio, which can be due to the stronger interaction between SPEEK and SBA-15 as shown in Scheme 2. The breaking strength of hybrid membranes firstly increases and then decreases, showing a highest value in S/SBA-15 5 membrane. With the increasing of SBA-15 mass ratio, the interaction between SPEEK and SBA-15 constantly increases, while the incompatibility between SPEEK matrix and SBA-15 inorganic particle also constantly increases which leads to weaker mechanical property of hybrid membranes. It seems that the two contradictory aspects together affect the breaking strength

Table 1
Physicochemical property, VO^{2+} permeability and mechanical property data of various membranes.

Membrane	Thickness (μm, wet)	Water uptake (%)	Swelling ratio (%)	IEC (mmol g^{-1})	Proton conductivity (mS cm^{-1})	VO^{2+} permeability (10^{-7} cm^2 min^{-1})	Breaking strength (MPa)	Young modulus (MPa)
Nafion 117	215	37.3	19.7	0.93	30.7	32.2	19.1	189
SPEEK	65	55.0	14.5	2.12	11.3	18.4	40.0	1045
S/SBA-15 5	52	47.7[a]/50.2[b]	13.2	2.03	10.9	14.5	44.8	1228
S/SBA-15 10	72	40.6[a]/45.1[b]	12.0	1.91	10.0	10.3	43.0	1409
S/SBA-15 15	64	35.8[a]/42.1[b]	8.8	1.82	8.8	8.0	42.8	1535
S/SBA-15 20	61	31.8[a]/39.8[b]	8.3	1.72	6.4	6.2	41.2	1635
S/SBA-15 25	62	30.0[a]/40.0[b]	7.7	1.65	3.8	7.9	36.3	1825

[a] The calculation of water uptake is based on the weight of the entire sample membrane.
[b] The calculation of water uptake is based on the weight of SPEEK content in sample membrane.

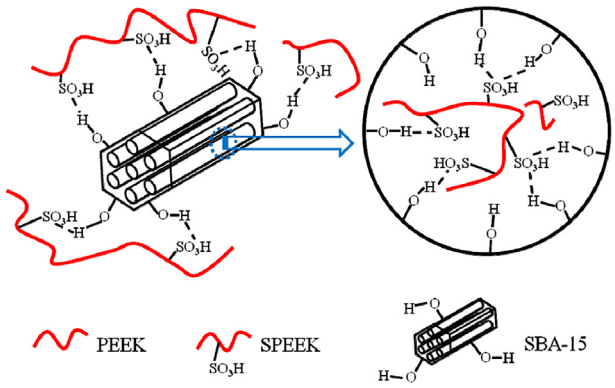

Scheme 2. The interaction mechanism between SPEEK and SBA-15.

of hybrid membranes, and the incompatibility aspect would be larger with the increasing of SBA-15 mass ratio. Thus the phenomenon of breaking strength could be explained.

The thermal stability of SPEEK and hybrid membranes is shown in Fig. 3. It can be seen that the remanent weight ratio of sample membranes increases with the increasing of SBA-15 mass ratio as shown in Fig. 3(a), which can be attributed to the high thermal stability of SBA-15. The thermal degradation of SPEEK and hybrid membranes begins approximately at 290 °C as shown in Fig. 3(b), which is similar to the values as elsewhere reported [47,48]. Two distinct weight loss steps of SPEEK and hybrid membranes can be observed, which is reflected by the two peaks in the differential thermogravimetric analysis (DTA) curve in separate temperature ranges. The first weight loss step is due to the splitting-off of sulfonic acid groups in the SPEEK polymer [47,48]. The second weight loss step, which begins in the range of 410–440 °C, is attributed to the decomposition of SPEEK polymer main chain. The hybrid membranes show the same good thermal stability with SPEEK at the first weight loss step. The temperatures of the second peak in DTA curves are 517, 518, 534 and 531 °C with the increasing of SBA-15 mass ratio, showing the best thermal stability in S/SBA-15 20 hybrid membrane. The enhancement of the thermal stability of hybrid membranes at the second weight loss step could be attributed to the filling mesoporous pores of SBA-15 with SPEEK as shown in Scheme 2, and the shape change of the first peak in DTA curves could be attributed to the hydrogen bond formed between SPEEK and SBA-15. In general, the result of TGA indicates that the introduction of SBA-15 into the membranes can improve the thermal stability of hybrid membranes accompanied with good trend with the increasing of SBA-15 mass ratio.

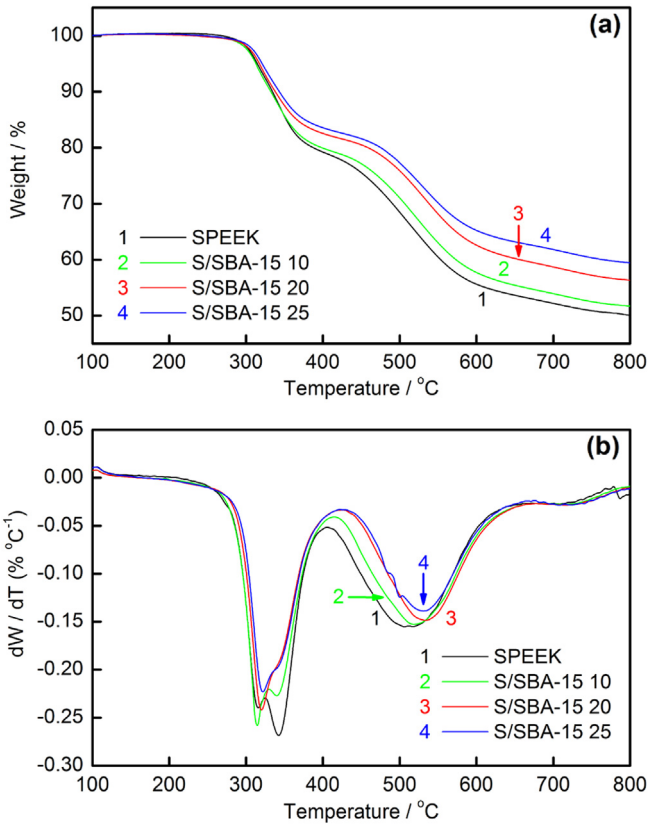

Fig. 3. TGA curves (a) and DTA curves (b) of SPEEK and hybrid membranes.

3.5. VRB single cell performance

As the results shown above, the S/SBA-15 hybrid membranes possess dense and homogeneous morphology, good trends of physicochemical property, VO^{2+} permeability, mechanical property, and thermal stability. Therefore, to further investigate the VRB single cell performance of S/SBA-15 hybrid membranes, the S/SBA-15 15, S/SBA-15 20 and S/SBA-15 25 membranes are selected to conduct the following tests accompanied with SPEEK and Nafion 117 membranes.

VRBs assembled with above-mentioned membranes respectively are utilized to conduct the charge–discharge tests at different current densities. The single cycle charge–discharge curves of these membranes at 60 mA cm^{-2} are illustrated in Fig. 4. The rank of charge–discharge time is S/SBA-15 20, SPEEK, S/SBA-15 15, S/SBA-15 25 and Nafion 117 membranes. The similar curves of S/SBA-15 15 and S/SBA-15 20 membranes are attributed to their similar properties, while the SPEEK membrane also can achieve the similar curve by the balance of relative high proton conductivity and vanadium ion permeability. The longest charge–discharge time possessed by S/SBA-15 20 membrane can be due to its good balance of proton conductivity and vanadium ion permeability, while the shorter charge–discharge time of S/SBA-15 25 membrane is owing to its lowest proton conductivity and larger resistance.

The result of coulombic efficiency (CE), voltage efficiency (VE) and energy efficiency (EE) at different current densities in the charge–discharge test with various membranes is demonstrated in Fig. 5. The rank of CE is S/SBA-15 25, S/SBA-15 20, S/SBA-15 15,

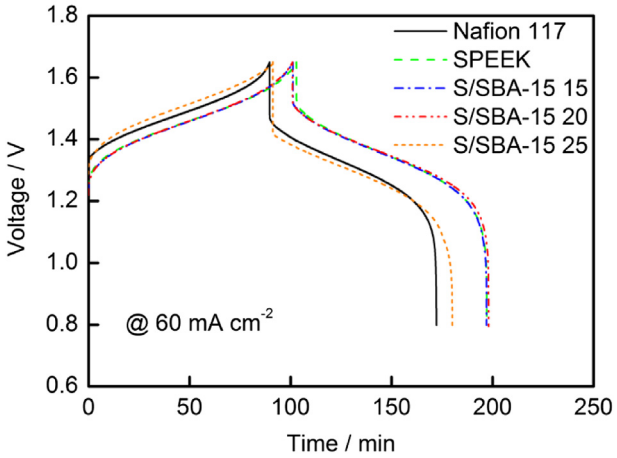

Fig. 4. Single cycle charge–discharge curves of VRBs assembled with various membranes at 60 mA cm^{-2}.

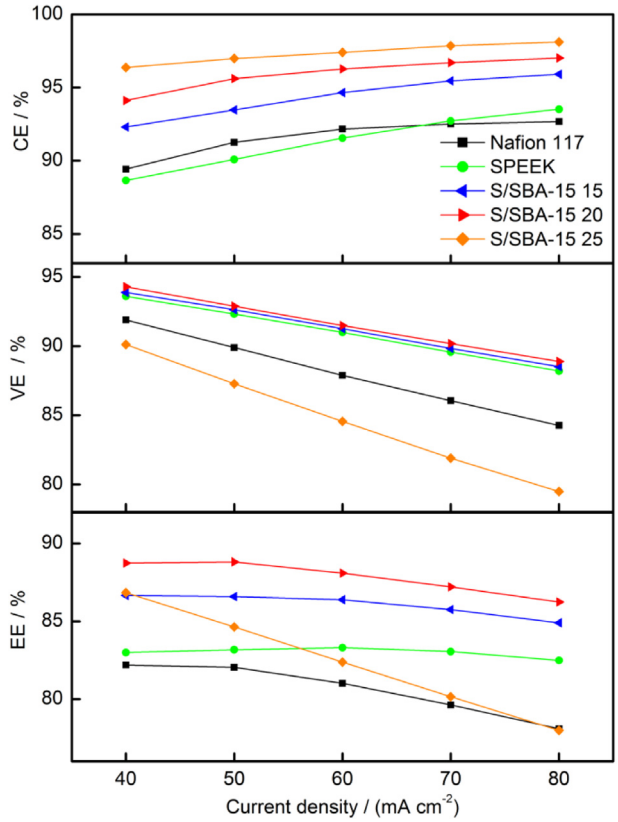

Fig. 5. Efficiency of VRBs assembled with various membranes from 40 to 80 mA cm^{-2} in the charge–discharge test.

SPEEK and Nafion 117 membranes at 70 and 80 mA cm^{-2}, which are in accordance with the VO^{2+} permeability results. With the increasing of SBA-15 mass ratio, the VO^{2+} permeability of hybrid membranes decreases, leading to less cross-mixed vanadium ions and higher CE. The rank of VE is S/SBA-15 20, S/SBA-15 15, SPEEK, Nafion 117 and S/SBA-15 25 membranes from 40 to 80 mA cm^{-2}, which agree well with the single cycle charge–discharge curves. As an important indicator, the EE reflects the energy conversion ability for large-scale VRB systems. The rank of EE is S/SBA-15 20, S/SBA-15 15, SPEEK and Nafion 117 membrane in all current densities except S/SBA-15 25 membrane. Owing to the lowest proton conductivity, the EE of S/SBA-15 25 membrane decreases rapidly with the increasing of current density for its larger resistance. Thus the S/SBA-15 25 membrane is not suitable using in high current density situation. Moreover, in this system, the S/SBA-15 20 membrane shows the best single cell performance of CE 96.3% and EE 88.1% at 60 mA cm^{-2}, while the Nafion 117 membrane shows the cell performance of CE 92.2% and EE 81.0%. In summary, to obtain better VRB performance, a balance between proton conductivity and vanadium ion permeability should be made via optimizing the mass ratio of SPEEK and SBA-15.

The single cell open circuit voltage (OCV) of VRBs assembled with various membranes in the self-discharge test is illustrated in Fig. 6. The OCV value gradually declines with time before reaching 1.25 V and then drops rapidly to 0.8 V. It can be seen that the self-discharge time of SPEEK, Nafion 117, S/SBA-15 15, S/SBA-15 20 and S/SBA-15 25 membranes are 41 h, 46 h, 53 h, 92 h and 71 h respectively, which generally agrees with the VO^{2+} permeability except SPEEK membrane. The SPEEK membrane possessed shorter self-discharge time than Nafion 117 membrane is owing to its much smaller membrane thickness and the half VO^{2+} permeability

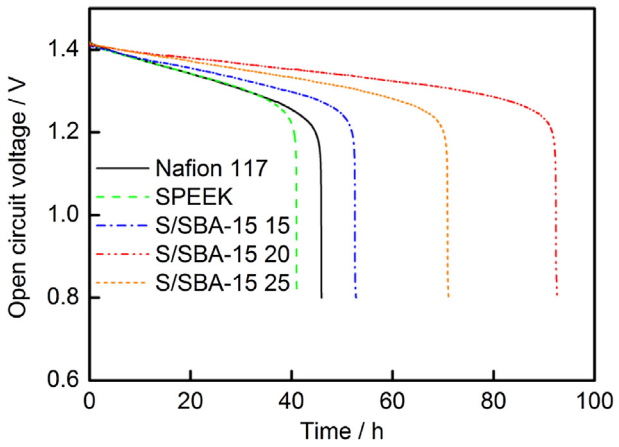

Fig. 6. Single cell open circuit voltage curves of VRBs assembled with various membranes.

compared with Nafion 117 membrane. These two factors together cause the shortest self-discharge time of SPEEK membrane in this system. Besides, the S/SBA-15 20 membrane possesses the longest self-discharge time due to its good balance of proton conductivity and VO^{2+} permeability.

As the results of charge–discharge test and self-discharge test demonstrated above, the S/SBA-15 20 membrane has the best VRB single cell performance of highest EE, longest charge–discharge time and self-discharge time. Therefore the cycle life test of VRBs assembled with S/SBA-15 20 and Nafion 117 membranes respectively is conducted at 60 mA cm^{-2} to evaluate the actual long-life stability of S/SBA-15 hybrid membranes. The cycle performances of these two membranes are illustrated in Fig. 7 (discharge capacity decline) and Fig. 8 (efficiency stability). The discharge capacity decline is owing to the unbalanced transports of vanadium ions and water, accompanied with some side reactions. As shown in Fig. 7, the S/SBA-15 20 membrane has higher discharge capacity remanent ratio than Nafion 117 membrane over 120 cycles, which can be due to its lower vanadium ion permeability. Furthermore, the discharge capacity remanent ratio of S/SBA-15 20 membrane decays a little faster after 40 cycles, which can be due to the increasing of hydrophilic domain in membrane and cross-mixed vanadium ions. After 120 cycles, the S/SBA-15 20 membrane still possesses 52% first cycle discharge capacity while the Nafion 117 membrane

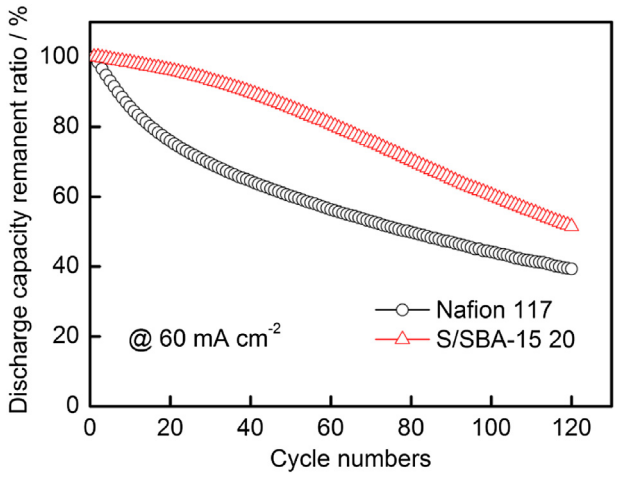

Fig. 7. Discharge capacity decline of VRBs assembled with Nafion 117 and S/SBA-15 20 membranes at 60 mA cm^{-2} in the cycle life test.

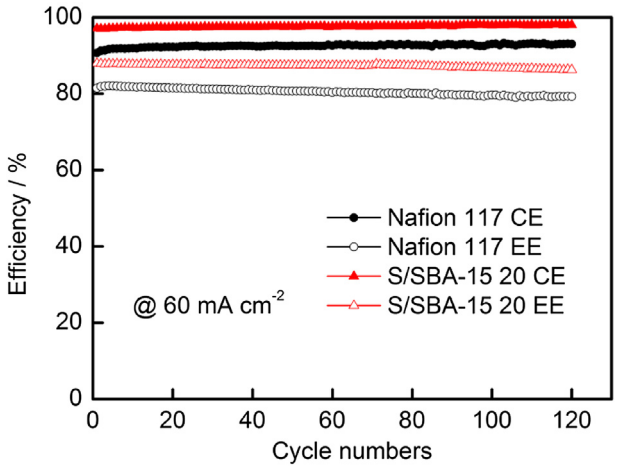

Fig. 8. Efficiency of VRBs assembled with Nafion 117 and S/SBA-15 20 membranes at 60 mA cm^{-2} in the cycle life test.

remains only 39%, which indicates that the S/SBA-15 20 membrane possesses higher stability than Nafion 117 membrane in this test. It can be seen that the CE and EE of VRBs assembled with these two membranes respectively are highly stable with no obvious decline over 120 cycles as shown in Fig. 8, which reveals that these two membranes have no fouling and damage causing the decreases of CE and EE. Besides, the values of CE and EE in cycle life test are consistent with the values in charge–discharge test, which shows the excellent repeatability of membrane preparation process. Overall, the cycle life test results reveal that the S/SBA-15 hybrid membranes exhibit high single cell performance and good stability in VRB.

With the above-mentioned discussions, the reason for higher and stable VRB performances of SPEEK/SBA-15 hybrid membranes could be summarized as follows. The addition of SBA-15 could decrease the water uptake and IEC of hybrid membranes, which would lead to lower proton conductivity, lower vanadium ion permeability and higher VRB performance. With the good balance of proton conductivity and vanadium ion permeability, the S/SBA-15 20 hybrid membrane shows the best VRB performance as above-mentioned results described. Besides, the addition of SBA-15 could also decrease the swelling ratio, which would lead to better mechanical property, better thermal stability, and stable VRB performance as the cycle life test results shown. Therefore, the SPEEK/SBA-15 hybrid membranes showing good performance could be considered as alternative low-cost membrane and used for VRB application.

4. Conclusions

The SPEEK/SBA-15 hybrid membranes are prepared by solution casting method with various SBA-15 mass ratios in this work. The cross-section morphology and EDX of the membranes are characterized, showing that the hybrid membranes are dense and homogeneous with no visible hole. With the increasing of SBA-15 mass ratio, the physicochemical property of hybrid membranes generally decreases accompanied with the explanations of filling SBA-15 mesoporous pores with SPEEK and the hydrogen bond formed between $-SO_3H$ group in SPEEK and $-OH$ group on SBA-15. Besides, the VO^{2+} permeability, mechanical property and thermal stability of hybrid membranes show good trends as the explanations described above. The single cell performance of VRBs assembled with the selected membranes, which are based on the results shown above, also represents excellent trend with the increasing of SBA-15 mass ratio. The S/SBA-15 20 membrane, which contains 20 wt.% SBA-15 in membrane matrix, shows the best VRB single cell performance of CE 96.3% and EE 88.1% at 60 mA cm^{-2} due to its good balance of proton conductivity and vanadium ion permeability. Furthermore, the cycle performance of VRB assembled with SPEEK/SBA-15 hybrid membrane is stable during 120 cycles accompanied with highly stable efficiency and slower discharge capacity decline. Therefore, the SPEEK/SBA-15 hybrid membranes with optimized mass ratio and excellent performance exhibit good potential usage in VRB systems.

Acknowledgments

This work was supported by the National Basic Research Program of China (2009CB220105, 2013CB934000), National Natural Science Foundation of China (21273129, 20973099), Shenzhen Science Fund for Distinguished Young Scholars (JC201104210149A) and Shenzhen Basic Research Project (CXZZ20130322164607310, JCYJ20130402145002403, and JCYJ20120830152316442).

References

[1] Z. Yang, J. Zhang, M.C.W. Kintner-Meyer, X. Lu, D. Choi, J.P. Lemmon, J. Liu, Chem. Rev. 111 (2011) 3577–3613.
[2] N. Armaroli, V. Balzani, Energy Environ. Sci. 4 (2011) 3193–3222.
[3] E. Sum, M. Skyllas-Kazacos, J. Power Sources 15 (1985) 179–190.
[4] E. Sum, M. Rychcik, M. Skyllas-kazacos, J. Power Sources 16 (1985) 85–95.
[5] M. Skyllas-Kazacos, M. Rychcik, R.G. Robins, A.G. Fane, M.A. Green, J. Electrochem. Soc. 133 (1986) 1057–1058.
[6] M. Skyllas-Kazacos, G. Kazacos, G. Poon, H. Verseema, Int. J. Energy Res. 34 (2010) 182–189.
[7] C.P. de León, A. Frías-Ferrer, J. González-García, D.A. Szánto, F.C. Walsh, J. Power Sources 160 (2006) 716–732.
[8] G. Kear, A.A. Shah, F.C. Walsh, Int. J. Energy Res. 36 (2012) 1105–1120.
[9] Parasuraman, T.M. Lim, C. Menictas, M. Skyllas-Kazacos, Electrochim. Acta 101 (2013) 27–40.
[10] X. Luo, Z. Lu, J. Xi, Z. Wu, W. Zhu, L. Chen, X. Qiu, J. Phys. Chem. B 109 (2005) 20310–20314.
[11] C. Yao, H. Zhang, T. Liu, X. Li, Z. Liu, J. Power Sources 237 (2013) 19–25.
[12] X. Liang, S. Peng, Y. Lei, C. Gao, N. Wang, S. Liu, D. Fang, Electrochim. Acta 95 (2013) 80–86.
[13] L. Li, S. Kim, W. Wang, M. Vijayakumar, Z. Nie, B. Chen, J. Zhang, G. Xia, J. Hu, G. Graff, J. Liu, Z. Yang, Adv. Energy Mater. 1 (2011) 394–400.
[14] W. Zhang, J. Xi, Z. Li, H. Zhou, L. Liu, Z. Wu, X. Qiu, Electrochim. Acta 89 (2013) 429–435.
[15] J. Xi, W. Zhang, Z. Li, H. Zhou, L. Liu, Z. Wu, X. Qiu, Int. J. Electrochem. Sci. 8 (2013) 4700–4711.
[16] G. Wei, J. Liu, H. Zhao, C. Yan, J. Power Sources 241 (2013) 709–717.
[17] Z. Li, J. Xi, H. Zhou, L. Liu, Z. Wu, X. Qiu, L. Chen, J. Power Sources 237 (2013) 132–140.
[18] D. Chen, S. Kim, V. Sprenkle, M.A. Hickner, J. Power Sources 231 (2013) 301–306.
[19] L. Liu, J. Xi, Z. Wu, W. Zhang, H. Zhou, W. Li, X. Qiu, J. Appl. Electrochem. 42 (2012) 1025–1031.
[20] A. Tang, S. Ting, J. Bao, M. Skyllas-Kazacos, J. Power Sources 203 (2012) 165–176.
[21] N. Wang, S. Peng, Y. Li, H. Wang, S. Liu, Y. Liu, J. Solid State Electrochem. 16 (2012) 2169–2177.
[22] J. Xi, Z. Wu, X. Qiu, L. Chen, J. Power Sources 166 (2007) 531–536.
[23] J. Xi, Z. Wu, X. Teng, Y. Zhao, L. Chen, X. Qiu, J. Mater. Chem. 18 (2008) 1232–1238.
[24] X. Teng, Y. Zhao, J. Xi, Z. Wu, X. Qiu, L. Chen, J. Membr. Sci. 341 (2009) 149–154.
[25] X. Teng, Y. Zhao, J. Xi, Z. Wu, X. Qiu, L. Chen, J. Power Sources 189 (2009) 1240–1246.
[26] Z. Mai, H. Zhang, X. Li, S. Xiao, H. Zhang, J. Power Sources 196 (2011) 5737–5741.
[27] N. Wang, S. Peng, D. Lu, S. Liu, Y. Liu, K. Huang, J. Solid State Electrochem. 16 (2012) 1577–1584.
[28] X. Teng, J. Dai, J. Su, Y. Zhu, H. Liu, Z. Song, J. Power Sources 240 (2013) 131–139.
[29] X. Teng, C. Sun, J. Dai, H. Liu, J. Su, F. Li, Electrochim. Acta 88 (2013) 725–734.
[30] H. Zhang, H. Zhang, X. Li, Z. Mai, J. Zhang, Energy Environ. Sci. 4 (2011) 1676–1679.
[31] Y. Li, H. Zhang, X. Li, H. Zhang, W. Wei, J. Power Sources 233 (2013) 202–208.
[32] X. Wei, L. Li, Q. Luo, Z. Nie, W. Wang, B. Li, G. Xia, E. Miller, J. Chambers, Z. Yang, J. Power Sources 218 (2012) 39–45.

[33] M.J. Jung, J. Parrondo, C.G. Arges, V. Ramani, J. Mater. Chem. A 1 (2013) 10458–10464.
[34] S. Zhang, B. Zhang, D. Xing, X. Jian, J. Mater. Chem. A 1 (2013) 12246–12254.
[35] Z. Mai, H. Zhang, H. Zhang, W. Xu, W. Wei, H. Na, X. Li, ChemSusChem 6 (2013) 328–335.
[36] D. Chen, M.A. Hickner, E. Agar, E.C. Kumbur, Appl. Mater. Interf. 5 (2013) 7559–7566.
[37] S. Kim, J. Yan, B. Schwenzer, J. Zhang, L. Li, J. Liu, Z. Yang, M.A. Hickner, Electrochem. Commun. 12 (2010) 1650–1653.
[38] X. Ling, C. Jia, J. Liu, C. Yan, J. Membr. Sci. 415–416 (2012) 306–312.
[39] D. Chen, S. Kim, L. Li, G. Yang, M.A. Hickner, RSC Adv. 2 (2012) 8087–8094.
[40] J. Pan, S. Wang, M. Xiao, M. Hickner, Y. Meng, J. Membr. Sci. 443 (2013) 19–27.
[41] N. Wang, J. Yu, Z. Zhou, D. Fang, S. Liu, Y. Liu, J. Membr. Sci. 437 (2013) 114–121.
[42] D. Zhao, J. Feng, Q. Huo, N. Melosh, G.H. Fredrickson, B.F. Chmelka, G.D. Stucky, Science 279 (1998) 548–552.
[43] Y. Wan, D. Zhao, Chem. Rev. 107 (2007) 2821–2860.
[44] J. Wootthikanokkhan, N. Seeponkai, J. Appl. Polym. Sci. 102 (2006) 5941–5947.
[45] J. Jarupatrakorn, T.D. Tilley, J. Am. Chem. Soc. 124 (2002) 8380–8388.
[46] K.D. Kreuer, J. Membr. Sci. 185 (2001) 29–39.
[47] S.M.J. Zaidi, S.D. Mikhailenko, G.P. Robertson, M.D. Guiver, S. Kaliaguine, J. Membr. Sci. 173 (2000) 17–34.
[48] M. Gil, X. Li, X. Li, H. Na, J.E. Hampsey, Y. Lu, J. Membr. Sci. 234 (2004) 75–81.